

9-8-1995

Work Function Dependence of Charge Transfer in Desorption and Sputtering of Atoms from Surfaces

Sarah J. Steuber
Rice University

Peter Nordlander
Rice University, nordland@surf.rice.edu

Hongxiao Shao
University of California, Santa Barbara

David C. Langreth
Rutgers University

Follow this and additional works at: <https://digitalcommons.usu.edu/microscopy>



Part of the [Biology Commons](#)

Recommended Citation

Steuber, Sarah J.; Nordlander, Peter; Shao, Hongxiao; and Langreth, David C. (1995) "Work Function Dependence of Charge Transfer in Desorption and Sputtering of Atoms from Surfaces," *Scanning Microscopy*: Vol. 9 : No. 3 , Article 2.

Available at: <https://digitalcommons.usu.edu/microscopy/vol9/iss3/2>

This Article is brought to you for free and open access by the Western Dairy Center at DigitalCommons@USU. It has been accepted for inclusion in Scanning Microscopy by an authorized administrator of DigitalCommons@USU. For more information, please contact digitalcommons@usu.edu.



WORK FUNCTION DEPENDENCE OF CHARGE TRANSFER IN DESORPTION AND SPUTTERING OF ATOMS FROM SURFACES

Sarah J. Steuber¹, Peter Nordlander^{1,*}, Hongxiao Shao², and David C. Langreth³

¹Department of Physics and Rice Quantum Institute, Rice University, Houston, Texas 77215-1892

²Quest, University of California, Santa Barbara, CA 93106

³Department of Physics and Astronomy, Rutgers University, Piscataway, NJ 08855-0849

(Received for publication May 21, 1995 and in revised form September 8, 1995)

Abstract

Using a recently developed many-electron theory, we investigate the work function dependence of charge transfer during desorption and sputtering of atoms from metal surfaces. We investigate the effects of substrate bandwidth, atomic velocity and level degeneracy on the charge transfer. We show that many-electron interactions introduce relatively small but measurable effects on the work function dependence of the charge transfer. We find that these effects can be stronger for negative ion states than for positive ion states. The reason is that for negative ions, a strongly correlated Kondo state may be formed near the surface.

Key Words: Charge transfer, tunneling, excited states, ion-surface scattering, desorption, sputtering.

Introduction

In recent years much research, both experimental and theoretical, involving the charge transfer processes of collisions between atoms or small molecules and surfaces has been performed [9, 11, 13, 14, 15]. An understanding of the charge transfer processes is important when events such as sticking and desorption are described. Theoretically, the problem is interesting because of the presence of relatively strong non-adiabatic, non-equilibrium, and electron-correlation effects. From an experimental point of view, the charge transfer process can be studied relatively straightforwardly for a very broad range of substrate and atomic parameters. By changing the substrate, properties such as bandwidth can be varied. The work function of the surface can be changed by adding varying amounts of impurities such as alkali atoms. The scattering atoms can be chosen according to what ion species and degeneracy are wanted. The velocity can also be controlled in a more trivial manner.

Until recently, most theoretical descriptions of charge transfer have been based on the time-independent, single level Anderson model [3, 4, 16, 25]. This model has proved to be insufficient to deal with the strong effects of degeneracy and intra-atomic correlation which are present in even the simplest cases, e.g., due to spin degeneracy. The fully time-dependent, multi-level and spin-dependent Hamiltonian, however, is very complicated and impossible to solve analytically even in equilibrium. Much work has been focused on finding approximate solutions to this problem [8, 21, 26, 31], and more recently, on the problems at the mesoscopic scale, in particular, the transport of electrons through quantum dots [5, 6, 12, 18, 20, 30, 32].

Recently, a general method was developed for the approximate solution of the time-dependent Anderson model using non-equilibrium Green's functions and the slave-boson method [17, 27]. It was shown that many-electron effects can strongly influence the charge transfer in atom surface scattering in typical situations. In a recent paper, the effects of many-electron interactions on

* Address for correspondence:

Peter Nordlander
Department of Physics,
Rice University,
P.O. Box 1892,
Houston, TX 77251-1892

Telephone number: (713) 285-5171

FAX number: (713) 527-9033

E.mail: nordland@surf.rice.edu

Table of Symbols

H	Hamiltonian
t	Time
σ	Electron spin
$\epsilon_{l\sigma}$	Atomic energy level
$n_{l\sigma}$	Population of atomic energy level
ϵ_k	Conduction electron energy level
$n_{k\sigma}$	Population of conduction energy level
U	Intra-atomic correlation energy
$V_{l\sigma k}$	Hopping matrix element
$ \alpha\rangle$	N-fold degenerate atomic energy level
n_α	Population of atomic energy level
N	Degeneracy of atomic energy level
$G_{l\sigma}$	Green's function for atomic level
$A_{l\sigma}$	Two-particle correlation function
G_α	Green's function for atomic level
A_α	Two-particle correlation function
B	Green's function for slave-boson
b	Slave boson correlation function
ρ_α^{OCC}	Occupied spectral density
T	Total time
τ	Difference time
ω	Frequency
ξ	Density of states
ϵ	Energy
D	Substrate half-bandwidth
ϵ_N	Atomic affinity energy
ϵ_P	Atomic ionization level
Φ	Energy level parameter
Z	Atom-surface separation
Γ_α	Width of atomic level
$\bar{\Gamma}_\alpha$	Band-averaged width of atomic level
Γ	Total width of atomic level
$\bar{\Gamma}$	Total band-averaged width of atomic level
$\bar{\Gamma}_\alpha^0$	Width parameter
ζ	Distance dependence of width of atomic level
f	Fermi-Dirac distribution function
Z_C	Level crossing distance
v	Velocity of atom
δn	Population deviation from adiabatic limit
T_K	Kondo temperature

the velocity dependence of charge transfer was investigated and it was shown that the final charge transfer probability, at low velocities, could be strongly enhanced in situations where electron-electron interaction induces a Kondo resonance [27].

The main focus of the present work is to study the influence of many-body interactions on the work function dependence of charge transfer. This dependence is one of the primary experimental quantities to be studied [7, 19]. We investigate how the work function dependence of charge transfer is influenced by degeneracy, atomic velocity and substrate bandwidth. The physical origin of the effects are investigated by analyzing the instantaneous spectral functions of the atomic levels. The results show that many-electron interactions cause small but measurable effects in the work function dependence of charge transfer in desorption and sputtering of atoms from surfaces. The results also indicate that many-electron effects play a much less prominent role for the work function dependence of charge transfer than they do for the velocity dependence [28] or for the substrate temperature dependence [29] of charge transfer.

Theory

The interaction between the atom and the surface is described using a time dependent Anderson Hamiltonian [1],

$$\begin{aligned}
 H(t) = & \sum_{l\sigma} \epsilon_{l\sigma}(t) n_{l\sigma} + \frac{1}{2} \sum' U_{l\sigma, l'\sigma'} n_{l\sigma} n_{l'\sigma'} \\
 & + \sum_{k\sigma} \epsilon_k n_{k\sigma} \\
 & + \sum_{l\sigma k} [V_{l\sigma k}(t) c_{k\sigma}^\dagger c_{l\sigma} + \text{H.c.}] .
 \end{aligned} \quad (1)$$

In this equation, the different atomic levels and $\epsilon_{l\sigma}(t)$ are the energies of the substrate electrons. The subscript σ denotes spin for both the atomic states and the conduction electrons; l and k , refer to the spatial quantum numbers of the atom and the metal's conduction electrons respectively. The components in l and k referring to a common symmetry for both the atom and metal are conserved [27]. The first summation describes the bare atomic states, the second describes intra-atomic correlation (the primed summation here excludes the term in which both $l = l'$ and $\sigma = \sigma'$). The third summation represents the surface conduction electrons, and the fourth summation describes the tunneling between the atomic states and the surface conduction band of the metal. The abbreviation H.c. denotes the Hermitian conjugate.

For simplicity, the present investigation will be limited to atoms characterized by a single N-fold degenerate

level. We will refer to this level as $|\alpha\rangle$. We assume a strong intra-atomic correlation term U , such that only single occupation of the N -fold degenerate level is possible. In this model, $N = 1$ corresponds to $U = 0$, i.e., the neglect of many-electron effects. For $N = 1$, the solution of eq. (1) is straightforward. For $N > 1$, the solution of eq. (1) is accomplished using the slave boson method and a non-equilibrium Green's function technique [17, 27, 28]. The instantaneous populations of one of the atomic levels are obtained from the equal time argument of the corresponding non-equilibrium Green's function, $n_\alpha^{\text{single}}(t) = G_\alpha^<(t, t)$. In the following, we will only be concerned with the total population of the atomic levels. For an N -fold degenerate atomic level, the atomic population is therefore obtained as

$$n_\alpha(t) = N G_\alpha^<(t, t') . \quad (2)$$

The instantaneous spectral functions presented in this work are calculated from the non-equal time argument of a two-particle correlation function

$$A_{I\sigma}^<(t, t') = G_{I\sigma}^<(t, t') b(t, t') , \quad (3)$$

where

$$b(t, t') = i [B^R(t', t) \theta(t' - t) - B^A(t', t) \theta(t - t')] , \quad (4)$$

where $B^{R/A}(t', t)$ is the retarded/advanced Green's function for the slave-boson. The Fourier transformation of this correlation function, using the new variables $T = 0.5(t + t')$ and $\tau = (t - t')$, is the total spectral density of occupied atomic states:

$$\rho_\alpha^{\text{occ}}(\omega, T) = \frac{N}{2\pi} \int_{-\infty}^{\infty} d\tau A_\alpha^<(T + \frac{\tau}{2}, T - \frac{\tau}{2}) \exp[i\omega\tau] . \quad (5)$$

As in eq. (2), the degeneracy of the atomic levels has been taken into account by the multiplication of N . The spectral function is the probability that an electron removed from state $|\alpha\rangle$ at time T will have an energy ω . The instantaneous population of the atomic levels can be obtained from the spectral function using

$$n_\alpha(T) = \int_{-\infty}^{\infty} d\omega \rho_\alpha^{\text{occ}}(\omega, T) . \quad (6)$$

The surface is modeled using the jellium model [22]

with a parabolic density of states which is described by:

$$\xi(\epsilon) = \frac{3}{2} \left(1 - \frac{\epsilon^2}{D^2} \right) \quad (7)$$

for $|\epsilon| < D$, and zero elsewhere. In this equation, D is the half-bandwidth of the substrate conduction band. In the investigations of the effect of substrate bandwidth on charge transfer presented below, D will be varied. The band is assumed half-filled and the energy scale is chosen such that the Fermi energy is at zero energy.

When an atom is near a metal surface, its energy levels will be shifted due to the image interaction [22]. In this paper, we will investigate the interaction of positive and negative ions levels with surfaces [27]. As far as the charge transfer dynamics is concerned, the relevant parameter is position of the atomic level with respect to the Fermi energy which is zero on our energy scale. A reasonable parameterization for the distance dependence of the level shift of the negative ion is [22],

$$\epsilon_N(t) = \phi - \frac{27.2}{4(Z(t) - 1)} \text{ eV} \quad (8)$$

and for the positive ion,

$$\epsilon_P(t) = -\phi + \frac{27.2}{4(Z(t) - 1)} \text{ eV} . \quad (9)$$

In these equations, $Z(t)$ is the distance from the jellium edge. The image plane is assumed to be located at $Z = 1$ a.u. The parameter Φ depends on the work function of the metal. For the negative ion, Φ is the difference between the energy of the atomic affinity level in vacuum and the Fermi energy of the substrate,

$$\phi = \epsilon_A - \epsilon_F . \quad (10)$$

For the positive ion, Φ is the difference between the Fermi energy and the energy of the atomic ionization level in vacuum,

$$\phi = \epsilon_F - \epsilon_I . \quad (11)$$

Atomic affinity and ionization levels of the common elements range from 0-8 eV. Metallic work functions range from 2-6 eV giving a range of Φ from -6 eV to 6 eV. In the calculations presented in this paper, we will only be interested in systems in which the atomic affinity or ionization level crosses the Fermi energy at some position outside the surface, i.e., $\Phi > 0$. In Figure 1, the energy shift of the positive and negative ion states are schematically indicated.

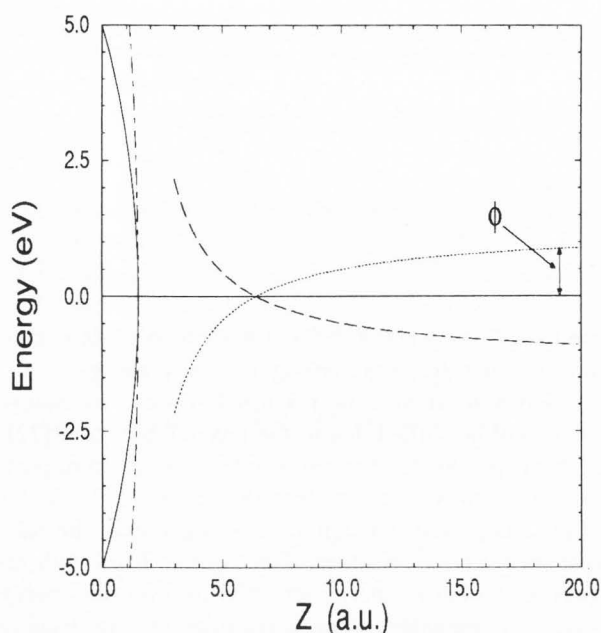


Figure 1. Schematic plot of the level shift as a function of atom surface separation. Dotted line is $\epsilon_N(Z)$, long-dashed line is $\epsilon_P(Z)$. The solid and dash-dotted lines represent the shape of the density of states for bandwidth $D = 5$ eV and $D = 10$ eV, respectively.

The widths of atomic levels typically increase exponentially with decreasing atom surface separation [22]. As discussed in previous work [27], the input which determines the tunneling rates involves a band average of the tunneling rates and substrate density of states. The parameterization for the band averaged width is:

$$\overline{\Gamma}_\alpha(t) = \overline{\Gamma}_\alpha^0 \exp[-\zeta Z(t)] . \quad (12)$$

In the present calculation, the adiabatic golden rule width of the atomic level, Γ_α is related to $\overline{\Gamma}_\alpha$ by

$$\Gamma_\alpha(t) = \overline{\Gamma}_\alpha^0 \xi(\epsilon(t)) . \quad (13)$$

The adiabatic width Γ_α is related to the hopping matrix elements $V_{\alpha k \sigma}$ in the Hamiltonian eq. (1) by

$$\Gamma_\alpha = 2\pi \sum_{k\sigma} |V_{\alpha k \sigma}|^2 \delta(\epsilon_\alpha - \epsilon_k) . \quad (14)$$

A detailed discussion of the relation between the adiabatic width Γ_α and $\overline{\Gamma}_\alpha$ can be found in Shao *et al.* [27]. As the degeneracy N varies, the tunneling rates between the individual atomic levels and the surface $\overline{\Gamma}_\alpha$ are scaled so that the total width Γ ,

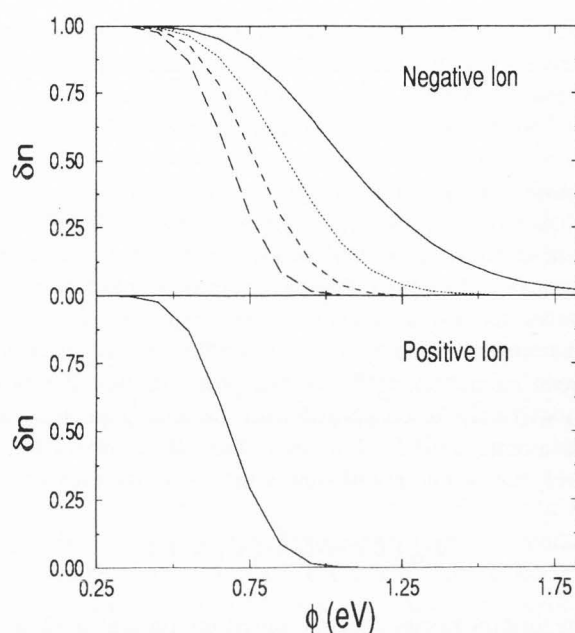


Figure 2. Simple master equation results for final population, $\delta n_N(\infty)$ and $\delta n_P(\infty)$ as a function of Φ , eqs. (10) and (11). The substrate bandwidth $D = 5$ eV. Solid line is for $N = 10$; dotted line $N = 4$; dashed line $N = 2$; and long-dashed line $N = 1$. The velocity of the atom is $v = 0.01$ a.u. Since $\delta n_P(\infty)$ is independent of degeneracy N , all curves lie on the same line.

$$\Gamma = \sum_{\alpha} \overline{\Gamma}_\alpha = N \overline{\Gamma}_\alpha , \quad (15)$$

is held constant. The calculations here were performed using $\zeta = 0.65$ a.u. and $\Gamma = 27.2$ eV for both positive and negative ions. The proposed parameterizations are realistic and appropriate for the interaction of the ionization levels and affinity levels of alkali atoms with free-electron metals such as Al or Cu [22, 23]. The substrate temperature in all calculations is 300K.

The calculations were performed using a trajectory in which the atom starts in its equilibrium configuration near the surface. At $t = 0$, the atom then starts to move away from the surface with constant velocity v . The equilibrium bond distance is assumed to be $Z = 3$ a.u. (from the jellium edge). None of the assumptions regarding the atomic trajectory or the atom/substrate parameters have any significant influence on the results of the calculations presented below.

Before applying the numerical Green's function method to calculate the charge transfer, it is useful to investigate the Φ and N dependence of the charge transfer using the simple master's equation (SME) [17, 24]. The

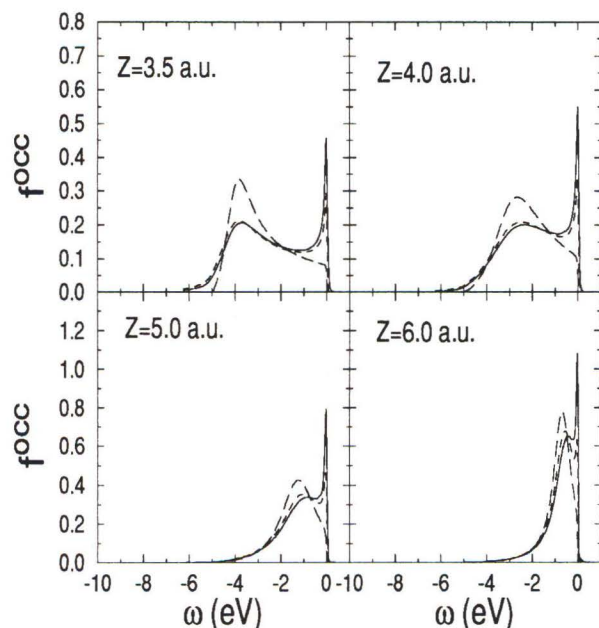


Figure 3. Degeneracy dependence of instantaneous spectral functions. The velocity $v = 0.005$ a.u., $\Phi = 0.75$ eV, the bandwidth $D = 5$ eV. Solid line is for $N = 10$; dashed line $N = 2$; and long-dashed line $N = 1$.

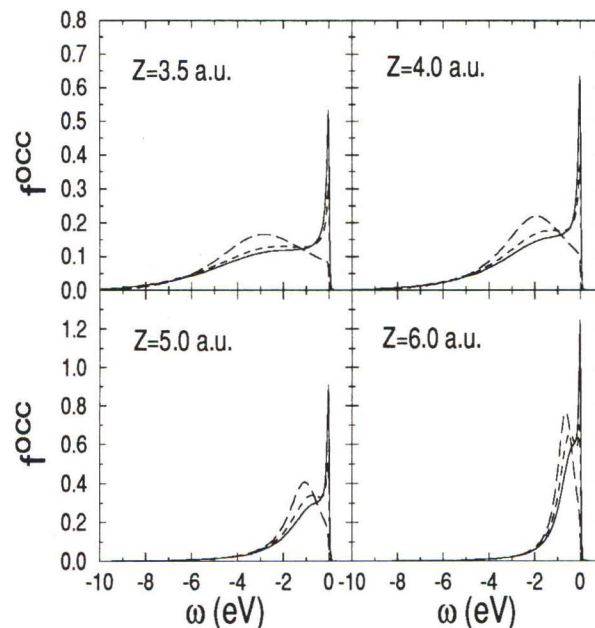


Figure 4. Degeneracy dependence of instantaneous spectral functions. The velocity $v = 0.005$ a.u., $\Phi = 0.75$ eV, bandwidth $D = 10$ eV. Solid line is for $N = 10$; dashed line $N = 2$; and long-dashed line $N = 1$.

SME provides a convenient method for a qualitative estimate of charge transfer probabilities in hyper-thermal atom surface scattering. The SME for this system has the form [17]

$$\frac{dn(t)}{dt} = \frac{-\Gamma(t)}{N} [1 - f(\epsilon(t))] + \Gamma(t) f(\epsilon(t)) [1 - n(t)], \quad (16)$$

where f is the Fermi function. Using the SME and assuming the temperature zero Kelvin we can calculate the population far from the surface. Using the initial conditions $n_N(Z_C) = 1$ and $n_P(Z_C) = 0$, where $Z_C = 27.2/4\Phi + 1$ is the distance, in a.u. (Bohr), when the atomic level crosses the Fermi energy, we obtain the results (for a rectangular substrate band),

$$\begin{aligned} n_N(a) &= \exp\left[\frac{-\Gamma(Z_C)}{\zeta v N}\right], \\ n_P(a) &= 1 - \exp\left[\frac{-\Gamma(Z_C)}{\zeta v}\right]. \end{aligned} \quad (17)$$

It can be seen that only for $N = 1$, $n_N(\infty) + n_P(\infty) = 1$. Because of the electron hole-pair symmetry for the $N = 1$ case, it is useful to plot $n_N(t)$ for the negative ion and $1 - n_P(t)$ for the positive ion. We therefore make the following definitions:

$$\delta n_N(t) = n_N(t), \quad \delta n_P(t) = 1 - n_P(t). \quad (18)$$

These quantities represent the deviations from adiabaticity since, for the work function presented in this work, the negative ion would have a population of zero far from the surface and the positive ion would have a population of unity, i.e., the atom would be neutral in both cases.

Figure 2 shows the results for positive and negative ions of different degeneracies for a substrate with a parabolic band. The solutions show several features of interest. First, we notice the strong work function dependence. As Φ increases, the crossing distance Z_C moves closer to the surface. The final population is therefore smaller for n_N and larger for n_P . Next, we notice that the negative ion has a strong N dependence. The N dependence comes from the rate at which the negative ion can depopulate. We see that a large degeneracy causes a slower tunneling rate and, therefore, a larger final population. For the positive ion, the SME predicts no N dependence. The solutions eq. (17) show a strong velocity dependence. As the velocity v approaches zero, $n_{N,P}(\infty)$, as a function of Φ , becomes steeper and eventually approaches a theta function centered at $\Phi = 0$. The numerical solution to eq. (16) shows no bandwidth dependence for $D > 5$ eV.

Results and Discussion

In the following, we will apply our many-body theory to the study of charge transfer as a function of substrate work function as represented by Φ , eqs. (10) and (11). In addition to the work function, many other parameters influence the charge transfer. To understand how each parameter affects the final population, we need to know what state the system is in at various points along the atom's trajectory. To do this, we will study the spectral functions of the system.

Spectral functions

Figures 3 and 4 show the instantaneous negative ion spectral functions for two different bandwidths at several distances from the surface for several values of N . For $N = 1$, the spectral function is characterized by an impurity peak centered around ϵ_α . The width of this peak is equal to Γ . For $N > 1$, an additional feature, the Kondo peak appears just below the Fermi energy.

The width of the Kondo peak, which is present in the spectral function for the degenerate atomic states (when electron correlation is included) is approximately equal to $2\pi T_K/N$. An analytical expression for the Kondo temperature has been derived and has the form [2, 10]

$$T_K = \frac{D}{2\pi} \exp\left[1.577 - \frac{3}{2N}\right] \cdot \left[\frac{\Gamma}{2\pi D}\right]^{\frac{1}{N}} \exp\left[2\pi \frac{|\epsilon_\alpha - \epsilon_F|}{\Gamma}\right]. \quad (19)$$

From this expression, it is clear that the Kondo peak will depend on bandwidth D , degeneracy N , and in particular, on the adiabatic position, ϵ_α , with respect to the Fermi level ϵ_F , and width of atomic level Γ .

Both the Kondo peak and the impurity peak are strongly influenced by the degeneracy. This degeneracy dependence comes from two sources. The height and the weight of the Kondo peak is determined partially by the Kondo temperature. In the present system, an increase of the bandwidth or degeneracy will increase T_K and the height and weight of the Kondo peak. The appearance of the Kondo peak in the system fundamentally changes the charge transfer dynamics. Since the Kondo peak, in general, is very narrow, non-adiabatic effects associated with the Kondo peak can be very pronounced, even at low velocities [28].

While the total population of the atomic level is relatively insensitive to N , the relative weight of the impurity and the Kondo peak changes with N . For $N = 1$, there is no Kondo peak, and the weight of the impurity peak is larger than for the $N > 1$ cases. Another difference in the impurity peaks is that for larger N , the

impurity peak is localized closer to the Fermi energy than for smaller N . This is particularly noticeable in the small bandwidth case which shows larger shifts than the large bandwidth case.

The energy shift of the impurity peak can be estimated using second order perturbation theory,

$$\Delta E_\alpha = \sum_k \frac{|V_{\alpha k}(t)|^2}{\epsilon_\alpha - \epsilon} \approx \int_{-D}^D d\epsilon \frac{\xi(\epsilon) \Gamma_\alpha(t)}{\epsilon_\alpha - \epsilon}. \quad (20)$$

where $\xi(\epsilon)$ is the shape function in eq. (7). For a rectangular shaped band, this integral can be evaluated analytically resulting in the following expression,

$$\Delta E_\alpha = \frac{\Gamma(t)}{N} \left[\left(1 - \frac{\epsilon_\alpha^2}{D^2}\right) \log \left| \frac{\epsilon_\alpha + D}{\epsilon_\alpha - D} \right| + 2 \frac{\epsilon_\alpha}{D} \right]. \quad (21)$$

This result shows that the energy shift is inversely proportional to N and that the shift becomes larger when ϵ_α approaches the band edge. For finite bandwidth, the impurity level is always shifted away from the Fermi energy. These results qualitatively explain the results shown in Figures 3 and 4.

We have shown that both the impurity and Kondo peaks are affected strongly by degeneracy as well as by bandwidth. For the case of $N = 1$, we notice that as the atom moves away from the surface the spectral functions for the two bandwidth cases become almost identical. This is because there is no Kondo peak and the shift of the impurity peak vanishes when the atomic level lies close to the Fermi energy. For the cases of $N > 1$ the bandwidth dependence of the Kondo peak affects the impurity peak even when the atomic energy level is close to the Fermi energy so the two bandwidth cases remain distinct.

All the spectral functions shown are for the negative ion case. The spectral functions for the positive ion case are very different [28]. Since the atomic energy level is above the Fermi energy when the atom is close to the surface there is no Kondo peak in the occupied spectral function. The occupied spectral weight is due to the tail of the impurity peak extending below the Fermi energy. Since in this limit, the width of the impurity peak is Γ/N , the population will be N -dependent. Since there is no Kondo peak, the bandwidth dependence is weak. At large atom surface separations, the atomic level shifts below the Fermi energy, and a Kondo resonance appears below the Fermi energy. However, since Γ is very

Work function dependence of charge transfer

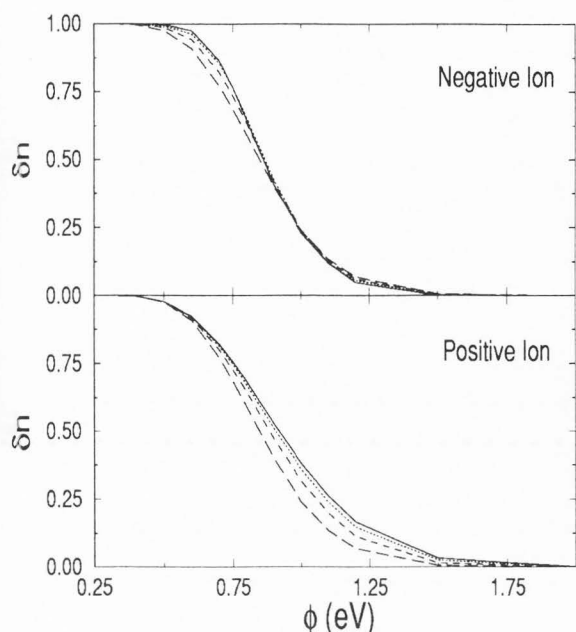


Figure 5. Work function dependence of $\delta n(\infty)$ for negative and positive ions. The velocity $v = 0.01$ a.u. Solid line is for $N = 10$; dotted line $N = 4$; dashed line $N = 2$; and long-dashed line $N = 1$.

small, T_K as given by eq. (19) will be very low. The Kondo peak therefore does not contribute to the occupied spectral function at room temperature.

Since both the bandwidth and degeneracy influence the spectral function when many-electron effects are included, we expect that the final population will be also influenced by the degeneracy and the bandwidth.

Influence of degeneracy

Figure 5 shows δn as a function of Φ for several different degeneracies for both positive and negative ions. By comparing Figure 5 with Figure 2, it can be seen that although both figures display the same general work function dependence, there are distinct differences. Figure 5 shows a strong degeneracy dependence which is different for the positive and negative ions. If electron correlation effects are neglected ($N = 1$), there is electron hole-pair symmetry and the positive and negative ion results are identical. The $N = 1$ results are very similar to the results from the SME. From Figure 5, we see that the $\delta n(\infty)$ versus Φ curve becomes steeper with higher degeneracy. This behavior is the opposite to what is predicted by the SME. We also see from Figure 5 that the slope of $\delta n_p(\infty)$ versus Φ decreases with increasing N , despite the fact that in the SME limit there is no degeneracy dependence.

A detailed explanation of the differences between the exact results and the results from the SME is beyond

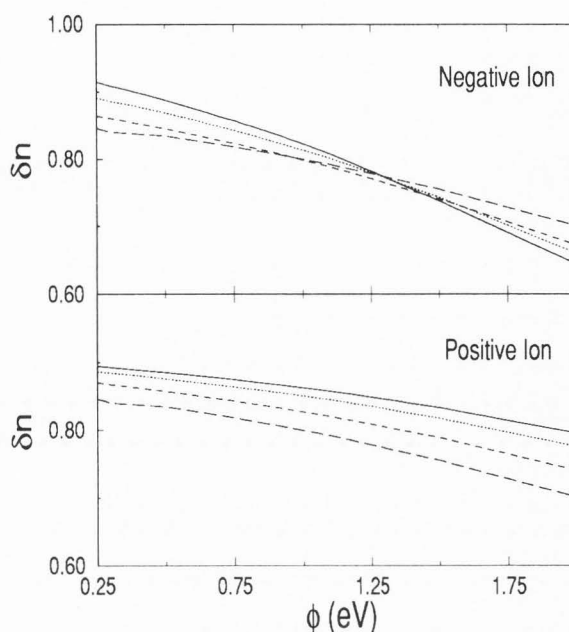


Figure 6. Work function dependence of $\delta n(0)$ for negative and positive ions. The bandwidth $D = 5$ eV. Solid line is for $N = 10$; dotted line $N = 4$; dashed line $N = 2$; and long-dashed line $N = 1$.

the scope of this paper. The SME limit includes many approximations, including the approximation that in equilibrium, when the atomic energy level lies above or below the Fermi energy, the level is completely empty or fully populated. This result is independent of degeneracy and substrate bandwidth. The Green's function solution on the other hand will depend on both the degeneracy and the substrate bandwidth. This can be seen in Figure 6, where the equilibrium populations of $\delta n_{N,p}(0)$ are plotted for the same parameters as in Figure 5. It can clearly be seen that the degeneracy dependence of the calculated $\delta n_{N,p}(0)$ as a function of work function closely parallels that in Figure 5. The correlation between $\delta n_{N,p}(\infty)$ and $\delta n_{N,p}(0)$ does not indicate that the $\delta n_{N,p}(\infty)$ depends on the particular initial condition chosen when solving the Dyson's equations. Neither do the results depend sensitively on $Z(0)$, provided $Z(0) < 4$ a.u. In the region near the surface, the population of the atom quickly adjusts to the equilibrium value.

The dependence of the equilibrium population $n_N(0)$ on degeneracy, bandwidth and work function is non-trivial and an extensive discussion has been published elsewhere [10]. The degeneracy and work function dependence of $\delta n_p(0)$ can be understood directly from the corresponding spectral function discussed in the previous subsection. The degeneracy dependence comes from the

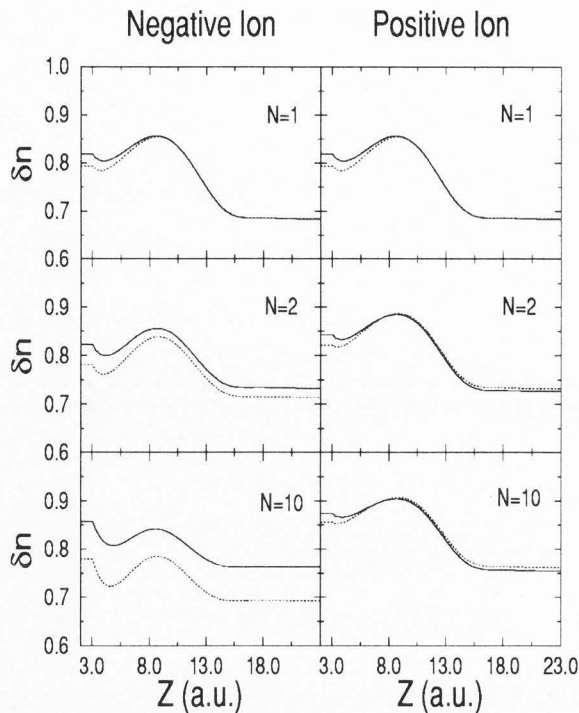


Figure 7. Instantaneous population for negative and positive ion. The velocity $v = 0.01$ a.u., $\Phi = 0.75$ eV. Solid line is for $D = 5$ eV, and dotted line $D = 10$ eV.

narrowing and shift of the impurity peak when the level lies above the Fermi energy. The work function dependence arises from the shift of the impurity peak with respect to the Fermi energy.

In Figure 7, the instantaneous population of the ion along its trajectory is plotted. The figure illustrates some of the complexity of the charge transfer. For both the positive and negative ion states, as the atom moves towards the vacuum, δn decreases. This is caused by the fact that when the atom recedes from the surface, the energy level approaches the Fermi level. For the negative ion state, this decreases the occupancy, and for the positive ion state, the occupancy is increased. At a distance of around $Z = 5$ a.u., δn begins to increase. This is primarily caused by the narrowing of the impurity peak. At a distance of $Z = 10$ a.u., the atomic levels cross the Fermi energy and $\delta n(Z)$ begins to decrease. The decrease in $\delta n(Z)$ continues until the atom-surface separation is so large that the tunneling rates becomes negligible.

We also see that most of the differences in the instantaneous populations occur before the impurity level crosses the Fermi energy. As discussed above, this is not an effect of the initial population but caused by the fact that the spectral distributions are relatively broad and sensitive to the atomic and substrate parameters in

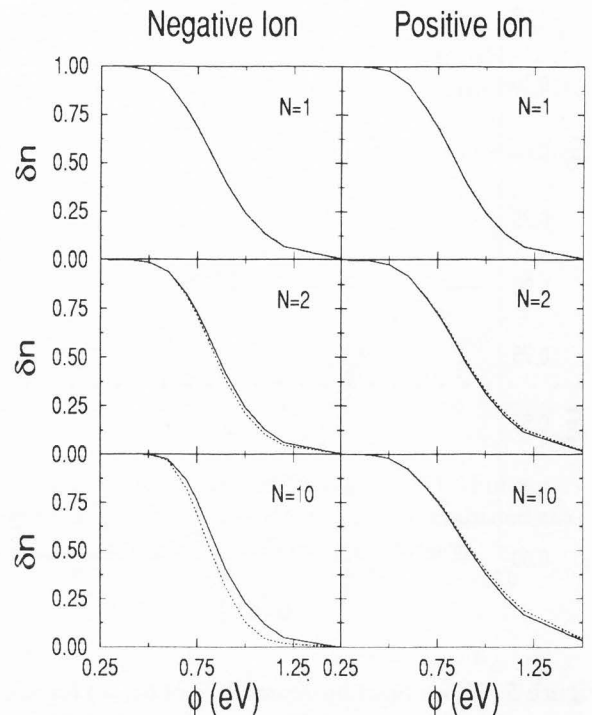


Figure 8. The plot of δn versus Φ for negative and positive ion. The velocity $v = 0.01$ a.u. Solid line is for $D = 5$ eV, and dotted line $D = 10$ eV.

this region. When the atomic level crosses the Fermi energy, the charge transfer is approximately as would be expected from the SME. It can clearly be seen from Figure 7 that for the negative ion, the neutralization rate decreases with increasing degeneracy. For the positive ion state, the neutralization rate is approximately independent of N .

Influence of substrate bandwidth

We have seen that the bandwidth of the substrate strongly affects the spectral function. Now, we examine how the bandwidth affects the final population. First, we examine the negative ion case. Figure 8 shows a comparison of $\delta n_N(\infty)$ versus Φ for two different bandwidths for several degeneracies. We see that for $N = 1$, the bandwidth has no significant effect on the final population. For $N > 1$, however, we see a distinct bandwidth dependence. This bandwidth dependence is caused by intra-atomic correlation effects, i.e., the Kondo peak.

Figure 7 shows the instantaneous population of the negative ion as it travels along its trajectory. We can see that for $N = 1$, the populations for both bandwidths merge around $Z = 10$ a.u., where the atomic level crosses the Fermi energy for $\Phi = 0.75$ eV. We also see that most of the differences in instantaneous populations occur before the impurity level crosses the Fermi

Work function dependence of charge transfer

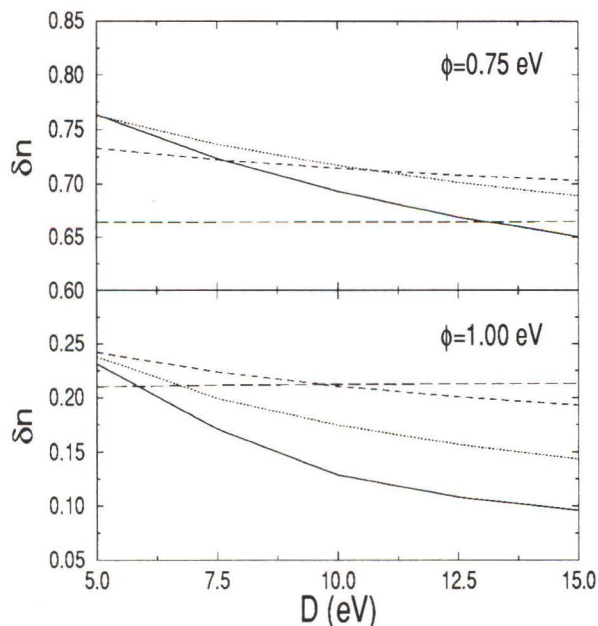


Figure 9. Bandwidth dependence of $\delta n(\infty)$ for negative ions. Solid line is for $N = 10$; dotted line $N = 4$; dashed line $N = 2$; and long-dashed line $N = 1$. The atomic velocity is $v = 0.01$ a.u.

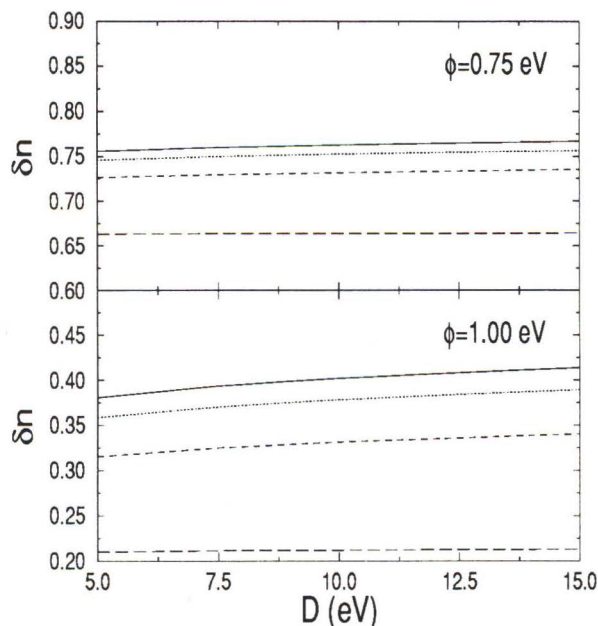


Figure 10. Bandwidth dependence of $\delta n(\infty)$ for positive ions. Solid line is for $N = 10$; dotted line $N = 4$; dashed line $N = 2$; and long-dashed line $N = 1$. The atomic velocity is $v = 0.01$ a.u.

energy. After the impurity level crosses the Fermi energy, both the small and the large bandwidth cases seem to lose the same amount of population for each N . The significant differences in the final population for $N > 1$ are, therefore, caused by the differences in the initial population for the two bandwidths. Since the neutralization rate is smaller for the larger degeneracies, the differences in final population are largest for large N .

Figure 8 shows $\delta n_P(\infty)$ as a function of work function for different N and different bandwidths. Only very small bandwidth differences can be seen. The major reason for this is that near the surface, the level lies above the Fermi energy. In this limit, the bandwidth dependence of the population is relatively weak. For the largest Φ , 1-1.5 eV, a slight bandwidth dependence can be observed in $n_P(\infty)$ because, for these work functions, the atomic level shifts below the Fermi level relatively close to the surface. When this happens, a small Kondo peak can be formed in the spectral function and the population becomes weakly bandwidth dependent.

From the plot of the instantaneous population $\delta n_P(t)$ in Figure 7, it can also be seen that the effects of substrate bandwidth are smaller for the positive ion than for the negative ion. As the atom moves towards the point where the positive ion state crosses the Fermi energy, the instantaneous populations of the atomic levels adjust

almost adiabatically. This process is efficient since the neutralization rate is independent of N and no Kondo peak is present. When the atomic level crosses the Fermi level, the bandwidth differences are of course minor.

In Figure 9, the bandwidth dependence of the final populations $\delta n_N(\infty)$ for the negative ion state is plotted as a function of bandwidth for two different work functions. If many-electron effects are neglected ($N = 1$), there is almost no effect of substrate bandwidth in the charge transfer. The situation changes drastically when intra-atomic correlation is included. For $N > 1$, the figure shows a strong bandwidth effect as discussed above. In Figure 10, $\delta n_P(\infty)$ as a function of bandwidth for the positive ion is shown for two different work functions. The bandwidth dependence is found to be very weak.

Influence of atomic velocity

In this section, we investigate the effects of velocity on $\delta n_{N,P}(\Phi)$. Figure 11 compares the δn results for various cases. We see that in each case, the slower velocity results show a steeper slope. This is expected since the slower an atom moves, the more time there is for the population to tunnel in or out of the surface. The steeper slope is also predicted by the SME eq. (16). Another

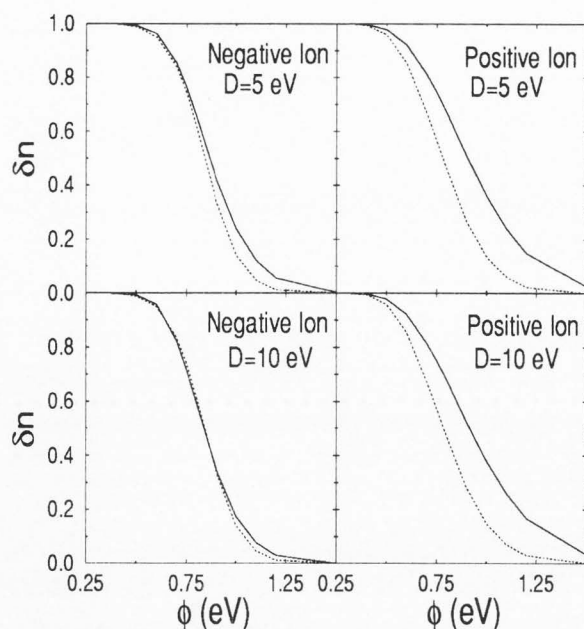


Figure 11. Velocity dependence of final population for $N = 4$. Solid line is for $v = 0.01$ a.u., and dotted line $v = 0.005$ a.u.

interesting feature is that for the negative ion the curves cross. This shows a fundamental difference between the positive ion and negative ion cases. For the positive ion, all final population decreased for decreasing velocity for all work functions. For the negative ion, we see that the velocity dependence of the system is very sensitive to which work function is chosen. For small Φ , the final population of the negative ions can increase with decreasing velocity. This is in direct contrast to the results of the SME which predicts a monotonic decrease in $\delta n_N(\infty)$ with decreasing N . This effect will be investigated in a future publication.

To see how the spectral functions are affected by velocity, the instantaneous spectral functions at certain atomic positions along the trajectory for $v = 0.005$ a.u. are plotted in Figure 12. For comparison, we also include the corresponding equilibrium ($v = 0$) spectral functions. We see that for $N = 1$, both spectral functions are nearly identical. The broad impurity peak forms very quickly and responds to the changing position of the atom almost immediately. When many-electron effects are included, the situation changes. For the case of $N = 4$, we see that the $v = 0.005$ and $v = 0$ spectral functions are very similar when the atom is close to the surface at $Z = 4$ a.u.; this is because the atom starts in equilibrium near the surface. As the atom moves away from the surface, the two spectral functions

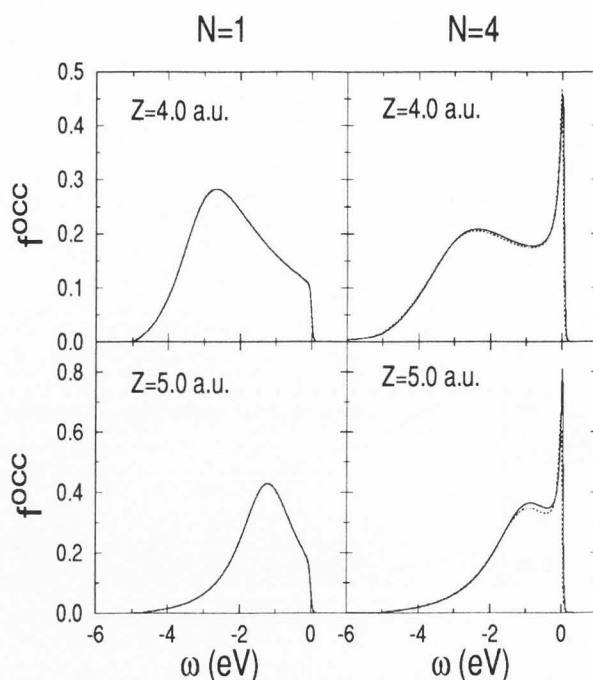


Figure 12. Velocity dependence of spectral functions. $\Phi = 0.75$ eV, the bandwidth $D = 5$ eV. Solid line is for $v = 0$ (equilibrium), and dotted line $v = 0.005$ a.u.

become different. For $Z = 6$ a.u., the $N = 4$ instantaneous spectral function has a smaller Kondo peak than the equilibrium spectral function. The atom is moving too fast to allow the Kondo peak to properly form.

The strong influence of many-electron effects on the charge transfer dynamics is caused by the different time-scales associated with the formation and decay the impurity peak and the Kondo peak. In a simple one-electron description, the charge transfer is controlled by the dynamics of the impurity peak. In real systems, the charge transfer also depends on the dynamics of Kondo resonance near the Fermi level.

Conclusions

We have shown that for a proper understanding of charge transfer using desorption or sputtering of atoms from surfaces, it is necessary to include many-electron effects. The calculated charge transfer as a function of work function depends on atomic degeneracy, substrate bandwidth and velocity in a manner that cannot be understood from simple rate equations. In particular, the negative ion species exhibit a nontrivial behavior. This is caused by the formation of a Kondo state when the atom is close to the surface. The predicted effect of bandwidth on charge transfer is sufficiently large that it could be measured experimentally.

Acknowledgement

This work is supported in part by the National Science Foundation under grants DMR 91-17479 (PN,SS) and DMR 94-07055 (DCL).

References

- [1] Anderson PW (1961) Localized magnetic states in metals. *Phys. Rev.* **124**: 41-58.
- [2] Bickers NE (1987) Review of techniques in the large-N expansion for dilute magnetic alloys. *Rev. Mod. Phys.* **59**: 845-939.
- [3] Blandin A, Nourtier A, Hone D (1976) Localised time-dependent perturbations in metals: Formalism and simple examples. *J. Physique* **37**: 369-378.
- [4] Brako R, Newns DM (1989) Theory of electronic processes in atom-surface scattering from surfaces. *Rep. Prog. Phys.* **52**: 655-697.
- [5] Bruder C, Schoeller H (1994) Charging effects in ultrasmall quantum dots in the presence of time-varying fields. *Phys. Rev. Lett.* **72**: 1076-1079.
- [6] Bryant GW (1993) Electrons in coupled vertical quantum dots: Interdot tunneling and Coulomb correlation. *Phys. Rev. B* **48**: 8024-8031.
- [7] Cooper BH, Behringer ER (1994) Scattering and Charge-transfer Dynamics. In: *Low Energy Ion-surface Interactions*. Rabalais J-W (ed.). John Wiley & Sons, Ltd., New York. pp. 263-312.
- [8] Goldberg EC, Flores F (1992) Charge exchange in many-body time-dependent processes. *Phys. Rev. B* **45**: 8657-8664.
- [9] Hammond MS, Dunning FB, Walters GK, Prinz GA (1992) Spin dependence in He(23S) metastable-atom de-excitation of magnetized Fe(110) and Fe(110) surfaces. *Phys. Rev. B* **45**: 3674-3683.
- [10] Hewson AC (1993) *The Kondo Problem to Heavy Fermions*. Cambridge University Press, Cambridge, U.K. pp. 171-231.
- [11] Hsu CC, Bu H, Bousetta A, Rabalais JW, Nordlander P (1992) Angular dependence of charge transfer probabilities between O- and a Ni{100}-c(2x2)-O surface. *Phys. Rev. Lett.* **69**: 188-191.
- [12] Jauho A-P, Wingreen NS, Meir Y (1994) Time-dependent transport in interacting and non-interacting resonant-tunneling systems. *Phys. Rev. B* **50**: 5528-5541.
- [13] Johnson AL, Joyce SA, Madey TE (1988) Electron-stimulated-desorption ion angular distributions of negative ions. *Phys. Rev. Lett.* **61**: 2578-2571.
- [14] Johnson PD, Viescas AJ, Nordlander P, Tully JC (1990) Formation of excited hydrogen states in stimulated desorption from an alkali-promoted surface. *Phys. Rev. Lett.* **64**: 942-945.
- [15] Kimmel GA, Goodstein FM, Levine ZH, Cooper BH (1991) Local adsorbate-induced effects on dynamical charge transfer in ion-surface scattering. *Phys. Rev. B* **43**: 9403-9412.
- [16] Lang ND (1983) Ionization probability of sputtered atoms. *Phys. Rev. B* **27**: 2019-2029.
- [17] Langreth DC, Nordlander P (1991) Derivation of a master equation for charge-transfer processes in atom-surface collisions. *Phys. Rev. B* **43**: 2541-2557.
- [18] Liu C, Niu Q (1993) Time-dependent Anderson model used to describe transport through quantum dots. *Phys. Rev. B* **47**: 13031-13046.
- [19] Los J, Geerlings JJC (1990) Charge exchange in atom-surface collisions. *Phys. Rep.* **190**: 133-190.
- [20] Maksym PA, Chakraborty T (1992) Quantum dots in a magnetic field: Role of electron-electron interactions. *Phys. Rev. Lett.* **65**: 108-111.
- [21] Marston JB, Andersson DR, Behringer ER, Cooper BH, Dirubio CA, Kimmel GA, Richardson C (1993) Many-body theory of charge transfer in hyperthermal atomic scattering. *Phys. Rev. B* **48**: 7809-7821.
- [22] Nordlander P, Tully JC (1990) Energy shifts and broadening of atomic levels near metal surfaces. *Phys. Rev. B* **42**: 5564-5578.
- [23] Nordlander P (1992) Lifetimes of negative-ion states near metal surfaces. *Phys. Rev. B* **46**: 2584-2590.
- [24] Nordlander P, Shao H, Langreth DC (1993) Intra-atomic correlation effects in charge-transfer. *Nucl. Instr. Meth. B* **78**: 11-19.
- [25] Norskov JK, Lundqvist BI (1979) Secondary ion emission probability in sputtering. *Phys. Rev. B* **19**: 5661-5665.
- [26] Sebastian KL (1985) Correlation effects in ion neutralization scattering with the use of a time-dependent coupled cluster approach. *Phys. Rev. B* **31**: 6976-6987.
- [27] Shao H, Langreth DC, Nordlander P (1994) Many-body theory for charge transfer in atom-surface collisions. *Phys. Rev. B* **49**: 13929-13947.
- [28] Shao H, Nordlander P, Langreth DC (1995) Non-adiabatic effects in charge transfer in atom-surface scattering. *Phys. Rev. B* **52**: 2988-2994.
- [29] H. Shao, P. Nordlander, D.C. Langreth. (1995). Non-adiabatic effects in charge transfer caused by electron-correlation. *Nucl. Instr. Meth. B* **100**: 261-266.
- [30] Stafford CA, Sarma SD (1994) Collective coulomb blockade in an array of quantum dots: A Mott-Hubbard approach. *Phys. Rev. Lett.* **72**: 3590-3593.
- [31] Sulston KW, Amos AT, Davison SG (1988) Many-electron theory of charge transfer in ion-surface scattering. *Phys. Rev. B* **37**: 9121-9129.
- [32] Wingreen NS, Meir Y (1994) Anderson model out of equilibrium: Noncrossing-approximation approach to transport through a quantum dot. *Phys. Rev. B* **49**: 11040-11053.

Discussion with Reviewers

F.J. Garcia de Abajo: Could you extrapolate on some of your conclusions to the case of an ion/surface system where Auger charge transfer processes are dominant?

Authors: The Auger transition probes the local density of states near the impinging atom. Many-electron effects similar to those discussed in the present paper are likely to also influence the Auger effects. However, since the Auger transition involves a self-convolution of the substrate band structure, features, such as, the Kondo peak, which is localized to a very narrow energy range near the Fermi surface, will tend to wash out.

F. Flores: Could you give some specific examples where the Kondo peak is expected to play a significant role on the ion states?

Authors: From an experimental point of view, many suitable atom/surface combination exists where the predicted effects could be measured. An example of systems where the Kondo resonance would contribute particularly strongly would be the alkaline earth metals scattered against noble metal surfaces. The ionization level of these atoms is a hole state and a strong Kondo resonance is expected to form near the surface [29]. Other interesting systems include oxygen or sulphur scattering on low work function surfaces.